

ChemComm

Accepted Manuscript



This is an *Accepted Manuscript*, which has been through the Royal Society of Chemistry peer review process and has been accepted for publication.

Accepted Manuscripts are published online shortly after acceptance, before technical editing, formatting and proof reading. Using this free service, authors can make their results available to the community, in citable form, before we publish the edited article. We will replace this *Accepted Manuscript* with the edited and formatted *Advance Article* as soon as it is available.

You can find more information about *Accepted Manuscripts* in the [Information for Authors](#).

Please note that technical editing may introduce minor changes to the text and/or graphics, which may alter content. The journal's standard [Terms & Conditions](#) and the [Ethical guidelines](#) still apply. In no event shall the Royal Society of Chemistry be held responsible for any errors or omissions in this *Accepted Manuscript* or any consequences arising from the use of any information it contains.



Chemical Communications

COMMUNICATION

Pro-aromatic Bisphenaleno-thieno[3,2-*b*]thiophene *versus* Anti-aromatic Bisindeno-thieno[3,2-*b*]thiophene: Different Ground-state Properties and Applications for Field-effect Transistors

Received 00th January 20xx,
Accepted 00th January 20xx

DOI: 10.1039/x0xx00000x

www.rsc.org/

Xueliang Shi,^a Sangsu Lee,^b Minjung Son,^b Bin Zheng,^c Jingjing Chang,^a Linzhi Jing,^a Kuo-Wei Huang,^c Dongho Kim^{b*} and Chunyan Chi^{a*}

A *pro-aromatic* bisphenaleno-thieno[3,2-*b*]thiophene (BPT-TIPS) was synthesized and compared with an *anti-aromatic* bisindeno-thieno[3,2-*b*]thiophene (S2-TIPS). BPT-TIPS showed larger diradical character, stronger absorption, longer excited state lifetime and better redox amphotericity than S2-TIPS.

Quinoidal π -conjugated molecules have recently attracted increasing interest due to their unique physical properties (low band gap and open-shell diradical character) and potential applications for field-effect transistors (FETs), non-linear optics, and spin-based electronics.¹ For this reason, various quinoidal polycyclic aromatic hydrocarbons (PAHs)² and their thiophene-based analogues³ have been synthesized and some of them have been successfully applied in ambipolar or *n*-channel FETs.⁴ In terms of such promising applications, fundamental understanding of how the fusion mode and the aromaticity/anti-aromaticity/pro-aromaticity affect the ground state electronic structure and consequently the physical properties is important. Recently, our group and Haley's group independently reported the synthesis and properties of a series of quinoidal bisindeno- $[n]$ thienoacenes (**Sn-TIPS**) ($n = 1-4$), which can be regarded as an *anti-aromatic* system containing an annulene framework with $4n$ π -electrons (Fig. 1).⁵ These molecules also displayed small to moderate diradical character in the ground state due to the recovery of the aromaticity of the central thienoacene moiety in the diradical form (Fig. 1). Analogues of this system are the bisphenaleno-thienoacenes in which the two indeno- units are replaced by two phenaleno- moieties, and the resulting quinoidal system is now *pro-aromatic* and an open-shell diradical resonance form can be drawn (Fig. 1). A comparison

between these two systems will provide insights into the correlations between the aromaticity, the ground state electronic structures, and the physical properties. Therefore, in this work, a *pro-aromatic* bisphenaleno-thieno[3,2-*b*]thiophene (**BPT-TIPS**) was synthesized and its ground state and physical properties were compared with its *anti-aromatic* counterpart, a bisindeno-thieno[3,2-*b*]thiophene (**S2-TIPS**) (Fig. 1). Our studies clearly show their distinctively different ground-state electronic structures and physical properties. Moreover, ordered 3D packing structure was observed in single crystals, qualifying **BPT-TIPS** as a new high performance semiconductor.

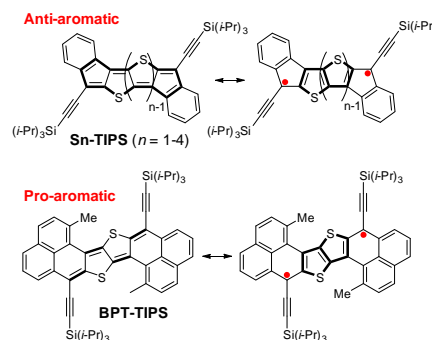


Fig. 1 Structures of anti-aromatic bisindeno-thienoacenes **Sn-TIPS** ($n = 1-4$) and *pro-aromatic* bisphenaleno-thieno[3,2-*b*]thiophene **BPT-TIPS**.

The key intermediate for the synthesis of **BPT-TIPS** was a α,α -di-ester substituted thieno[3,2-*b*]thiophene (TT) (**2**), which was obtained by regio-selective lithiation of 2,3,5,6-tetrabromo- TT (**1**) followed by quenching with methyl cyanofornate (Scheme 1). Suzuki coupling between **2** and (2-methylnaphthalen-1-yl)boronic acid gave **3** in 55% yield. Hydrolysis of **3** followed by acidification gave the diacid **4** in almost quantitative yield, which was converted into the corresponding carboxylic acid chloride with thionyl chloride in dry CH_2Cl_2 . Subsequent double Friedel-Crafts acylation with AlCl_3 afforded the desired diketone **5** in 85% yield. Finally, addition of triisopropylsilyl ethynyl lithium to the diketone **5**

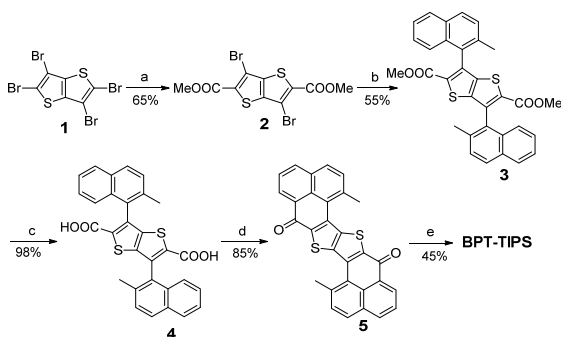
^a Department of Chemistry, National University of Singapore, 3 Science Drive 3, Singapore, 117543; E-mail: chmcc@nus.edu.sg (C.C.)

^b Spectroscopy Laboratory for Functional π -Electronic Systems and Department of Chemistry, Yonsei University, Seoul 120-749, Korea; E-mail: dongho@yonsei.ac.kr

^c KAUST Catalysis Center and Division of Physical Sciences & Engineering, King Abdullah University of Science and Technology (KAUST), Thuwal 23955-6900, Saudi Arabia

† Electronic Supplementary Information (ESI) available: Synthetic procedures and structural characterization data; additional physical characterization data; DFT calculations details. See DOI: 10.1039/x0xx00000x

and reduction of the intermediate diols by SnCl_2 gave the targeted compound **BPT-TIPS** in 45% yield.



Scheme 1. Synthetic route of **BPT-TIPS**: (a) i) $n\text{-BuLi}$, THF, -78°C , 1 h; ii) NC-COOMe , -78°C – r.t., overnight; (b) (2-methylnaphthalen-1-yl)boronic acid (4 equiv.), $\text{Pd}(\text{PPh}_3)_4/\text{K}_2\text{CO}_3$, toluene/EtOH/water (3:1:1), one drop aliquot 336, reflux, overnight; (c) i) NaOH , MeOH/THF (1:1), reflux overnight; ii) 10% HCl (aq.); (d) i) SOCl_2 , dry CH_2Cl_2 , reflux; ii) AlCl_3 , dry CH_2Cl_2 , 0°C – r.t., overnight; (e) i) triisopropylsilyl ethynyl lithium, THF, 0°C – r.t.; ii) SnCl_2 , toluene, r.t., 12 h.

BPT-TIPS exhibits good solubility and stability, displaying a blue colour in CH_2Cl_2 , while **S2-TIPS** exhibits a deep green colour (Fig. 2a). Additionally, **BPT-TIPS** shows a well-resolved absorption spectrum in CH_2Cl_2 with an intense p -band at 682 nm ($\log \epsilon = 5.03$; ϵ : molar extinction coefficient in $\text{M}^{-1} \text{cm}^{-1}$), which is commonly observed in many closed-shell PAHs such as acenes⁶ and closed-shell quinoidal compounds such as heptazethrene.^{2b} Therefore, this observation indicates that **BPT-TIPS** likely has a closed-shell electronic structure in the ground state. **S2-TIPS** exhibits a very different absorption spectrum with a broad the-longest-wavelength absorption band centered at 606 nm with much weaker intensity than that of **BPT-TIPS**, in accordance with its anti-aromatic character. Femtosecond transient absorption (TA) measurement was conducted to explore the excited-state dynamics of **BPT-TIPS** in toluene. The TA spectra exhibit ground-state bleach signal around 690 nm and a broad weak excited-state absorption band in 450–600 nm region (Fig. S1 in ESI[†]). The singlet excited-state lifetime (τ) was estimated to be 5.3 ns, which is much longer than that of the anti-aromatic **S2-TIPS** ($\tau_1 = 1.1$ ps, $\tau_2 = 10$ ps).^{5b} Moreover, two-photon absorption (TPA) measurements were also conducted for **BPT-TIPS** in toluene by the Z-scan technique in the NIR region from 1300 to 1500 nm (Fig. S2 in ESI[†]) and a maximum TPA cross section value ($\sigma_{\text{max}}^{(2)}$) of 620 GM (λ_{ex} : 1400 nm) was obtained, which is slightly higher than that for **S2-TIPS** ($\sigma_{\text{max}}^{(2)} = 520$ GM, λ_{ex} : 1400 nm) under the same condition.^{5b}

BPT-TIPS displays excellent amphoteric redox behavior with two reversible oxidation waves ($E_{1/2}^{\text{ox}} = -0.03, +0.44$ V vs Fc^+/Fc) and two reversible reduction waves ($E_{1/2}^{\text{red}} = -1.73, -1.38$ V vs Fc^+/Fc) (Fig. 2b). The HOMO and LUMO energy levels were estimated to be -4.65 eV and -3.46 eV from the onset of the first oxidation and reduction wave, respectively. While the anti-aromatic **S2-TIPS** which has a HOMO/LUMO level of $-5.35/-3.75$ eV ($E_g = 1.60$ eV) is easily reduced but hard to be oxidized, the pro-aromatic **BPT-TIPS** can be easily oxidized and

reduced to the corresponding radical cations/anions and dications/dianions, respectively. Such difference can be explained by the aromatic nature of both the cationic and anionic forms of **BPT-TIPS**, but for **S2-TIPS** its cationic forms are unstable due to the anti-aromatic nature of the cyclopentadienyl cation while its anionic forms are stable due to the aromatic character of the cyclopentadienyl anion.

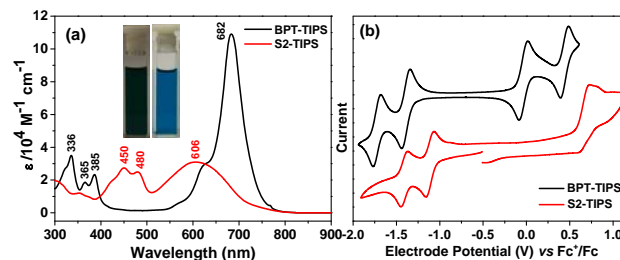


Fig. 2. (a) Electronic absorption spectra of **BPT-TIPS** and **S2-TIPS** in CH_2Cl_2 ; insert are the photos for the solutions of **S2-TIPS** (left) and **BPT-TIPS** (right). (b) Cyclic voltammograms of **BPT-TIPS** and **S2-TIPS** in CH_2Cl_2 containing 0.1 M TBAPF_6 .

The broken symmetry DFT calculation (UCAM-B3LYP/6-31G*) predicted that **BPT-TIPS** has an open-shell singlet diradical ground state, but with a small diradical character ($\gamma = 18.6\%$) and a large singlet-triplet energy gap ($E_{S-T} = -13.3$ kcal/mol). Such a small diradical character was not observed experimentally, and **BPT-TIPS** showed sharp NMR spectra even at elevated temperatures and was found ESR silent, suggesting a more closed-shell configuration of the ground state. With the same computation method, **S2-TIPS** was predicted to be a typical closed-shell system with a negligible diradical character. X-ray crystallographic analysis of **BPT-TIPS** (at 100 K) further elaborated their ground-state geometry (Fig. 3).[†] The molecule is distorted from planarity due to the repulsion between the methyl groups and the TT unit (Fig. 3a). Large bond length alternation was found in the central TT-quinodimethane moiety of both **BPT-TIPS** (Fig. 3b) and **S2-TIPS**,^{5b} indicating that closed-shell quinoidal form contributes most to the ground-state structure in both cases. However, NICS(1)zz calculations distinguished their different electronic structures. For **BPT-TIPS**, the NICS(1)zz values for the central two rings A and B are negative but much less negative than the outmost two rings C and D, indicating a small aromatic character of the rings A and B which can be correlated with its intrinsic pro-aromaticity. In contrast, the central two rings A and B in **S2-TIPS** possess positive NICS(1)zz values, implying a typical anti-aromatic character. **BPT-TIPS** can be also regarded as an isoelectronic structure of an octazethrene analogue (**OZ-TIPS**),^{2b} which has a larger diradical character due to the larger resonance energy of naphthalene spacer than thieno[3,2-*b*]acene.

Molecules of **BPT-TIPS** are packed into a 1D infinite head-to-tail chain with a short average π -stacking distance of 3.34 Å (Fig. 3c). The top view shows that the stacking is through phenalenyl-phenalenyl interaction, which is similar to the multi-center covalent bonding in the biphenalenyls,^{2a} but the distance is in the typical π - π stacking distance range (3.3–3.6 Å). Spin density distribution of the singlet diradical of **BPT-TIPS** shows that the spins are evenly distributed along the whole π -conjugated framework (Fig. S3 in ESI[†]), which thus explains the

decreased covalent character of the phenalenyl-phenalenyl interactions. The 1D polymer chains are then further stacked into a compact 3D network (side view, Fig. 3c), which is desirable for efficient charge transport.

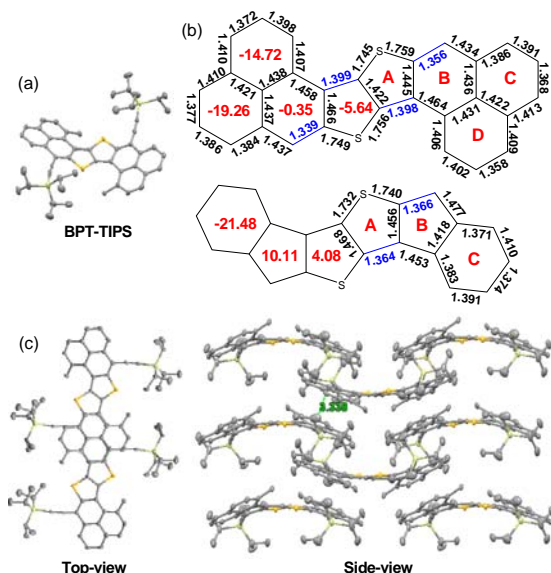


Fig. 3 (a) X-ray crystallographic structure of **BPT-TIPS**, hydrogen atoms are omitted for clearance; (b) selected bond length analysis from the single-crystal structures and calculated NICS(1)zz values (red numbers); (c) 3D packing structure of **BPT-TIPS**.

Bottom-gate, top-contact FETs were thus fabricated and used to evaluate the charge transporting properties of **BPT-TIPS** in both drop-casted and spin-coated thin films (ESI[†]). All the devices exhibited *p*-type operation with well-defined saturation behavior in nitrogen (Fig. S4 in ESI[†]). An average field effect hole mobility of $0.14 \text{ cm}^2 \text{V}^{-1} \text{s}^{-1}$ with a threshold voltage (V_{th}) of 4 V and a current on/off ratio of 10^4 were measured for the spin-coated thin films on OTS modified substrates (Table S2 in ESI[†]). When processed with drop casting method, large crystal domain was achieved, and as a result, the hole mobility was improved to be $0.26 \text{ cm}^2 \text{V}^{-1} \text{s}^{-1}$ almost without shifting the V_{th} . The different performance can be further correlated with the small surface roughness of the drop-casted thin films as revealed by optical microscope and atom force microscope measurements (Fig. S5-7 in ESI[†]). The XRD data in both drop-casted and spin-coated thin films indicate that the **BPT-TIPS** molecule has a similar layer-like packing to that of its single crystal (Fig. S8-9 in ESI[†]). Under similar processing conditions, the thin films of **S2-TIPS** showed much lower field-effect hole mobility ($0.016 \text{ cm}^2 \text{V}^{-1} \text{s}^{-1}$), which presumably can be ascribed to its separated columnar superstructure observed in the single crystals.^{5b}

In summary, we demonstrate that the quinoidal **BPT-TIPS** has distinctively different ground-state electronic structure and physical properties from its analogue **S2-TIPS**, which can be correlated with their respective pro-aromatic and anti-aromatic character. Our studies indicate that a pro-aromatic system exhibits a larger diradical character, stronger absorption, longer excited state lifetime and better redox

amphotericity than its anti-aromatic counterpart, which is important for future molecular design. The 3D ordered packing structure of this type of diradicaloid molecule led to a relatively high charge carrier mobility, which also paved the way to design materials for spin-dependent charge transport studies in next stage.

The work in NUS was supported by MOE Tier 1 grant (R-143-000-573-112), Tier 2 grant (MOE2014-T2-1-080) and Tier 3 programme (MOE2014-T3-1-004). The work at Yonsei University was supported by the Global Frontier R&D Program on Center for Multiscale Energy System funded by the National Research Foundation under the Ministry of Science, ICT & Future, Korea (NRF-2014M3A6A7060583). K. H. acknowledges financial support from KAUST. We thank Dr. Bruno Donnadiu for crystallographic analysis.

Notes and references

† Crystallographic data for **BPT-TIPS**: $\text{C}_{52}\text{H}_{54}\text{S}_2\text{Si}_2$. $M = 799.25$, monoclinic, $a = 17.7574(16) \text{ \AA}$, $b = 14.7085(14) \text{ \AA}$, $c = 17.0416(15) \text{ \AA}$, $\alpha = 90^\circ$, $\beta = 90.251(5)^\circ$, $\gamma = 90^\circ$, $V = 4451.0(7) \text{ \AA}^3$, $T = 100(2) \text{ K}$, space group $P 21/c$, $Z = 4$, CuK_α radiation $\lambda = 1.54178 \text{ \AA}$, $R_1 = 0.0770$ ($I > 2\sigma(I)$), $wR(F^2) = 0.2043$ ($I > 2\sigma(I)$); $R_1 = 0.1048$ (all data), $wR(F^2) = 0.2471$ (all data). CCDC No: 1055932.

- (a) Z. Sun, Q. Ye, C. Chi and J. Wu, *Chem. Soc. Rev.* 2012, **41**, 7857; (b) M. Abe, *Chem. Rev.* 2013, **113**, 7011; (c) Z. Sun, Z. Zeng and J. Wu, *Acc. Chem. Res.* 2014, **47**, 2582; (d) T. Kubo, *Chem. Rec.*, 2015, **15**, 218.
- Representative examples: (a) A. Shimizu, T. Kubo, M. Uruichi, K. Yakushi, M. Nakano, D. Shiomi, K. Sato, T. Takui, Y. Hirao, K. Matsumoto, H. Kurata, Y. Morita and K. Nakasuji, *J. Am. Chem. Soc.* 2010, **132**, 14421; (b) Y. Li, K.-W. Heng, B. S. Lee, N. Aratani, J. L. Zafra, N. Bao, R. Lee, Y. M. Sung, Z. Sun, K.-W. Huang, R. D. Webster, J. T. López Navarrete, D. Kim, A. Osuka, J. Casado, J. Ding and J. Wu, *J. Am. Chem. Soc.*, 2012, **134**, 14913; (c) D. T. Chase, B. D. Rose, S. P. McClintock, L. N. Zakharov and M. M. Haley, *Angew. Chem. Int. Ed.*, 2011, **50**, 1127; (d) A. Shimizu, R. Kishi, M. Nakano, D. Shiomi, K. Sato, T. Takui, I. Hisaki, M. Miyata and Y. Tobe, *Angew. Chem. Int. Ed.*, 2013, **52**, 6076; (e) Z. Zeng, S. Lee, J. L. Zafra, M. Ishida, X. Zhu, Z. Sun, Y. Ni, R. D. Webster, R.-W. Li, J. T. López Navarrete, C. Chi, J. Ding, J. Casado, D. Kim and J. Wu, *Angew. Chem. Int. Ed.*, 2013, **52**, 8561; (f) X. Yang, X.; D. Liu and Q. Miao, *Angew. Chem. Int. Ed.*, 2014, **53**, 6786.
- (a) T. Takahashi, K. I. Matsuoka, K. Takimiya, T. Otsubo and Y. Aso, *J. Am. Chem. Soc.*, 2005, **127**, 8928; (b) J. Casado, R. P. Ortiz and J. T. López Navarrete, *Chem. Soc. Rev.*, 2012, **41**, 5672.
- (a) T. M. Pappenfus, R. J. Chesterfield, C. D. Frisbie, K. R. Mann, J. Casado, J. D. Raff, and L. L. Miller, *J. Am. Chem. Soc.*, 2002, **124**, 4184; (b) R. J. Chesterfield, C. R. Newman, T. M. Pappenfus, P. C. Ewbank, M. H. Haukaas, K. R. Mann, L. L. Miller and C. D. Frisbie, *Adv. Mater.*, 2003, **15**, 1278; (c) Y. Suzuki, E. Miyazaki and K. Takimiya, *J. Am. Chem. Soc.*, 2010, **132**, 10453; (d) Q. Wu, R. Li, W. Hong, H. Li, X. Gao and D. Zhu, *Chem. Mater.*, 2011, **23**, 3138.
- (a) G. E. Rudebusch, A. G. Fix, H. A. Henthorn, C. L. Vonnegut, L. N. Zakharov and M. M. Haley, *Chem. Sci.*, 2014, **5**, 3627; (b) X. Shi, P. M. Burrezo, S. Lee, W. Zhang, B. Zheng, G. Dai, J. Chang, J. T. López Navarrete, K.-W. Huang, D. Kim, J. Casado and C. Chi, *Chem. Sci.*, 2014, **5**, 4490.
- J. E. Anthony, *Angew. Chem. Int. Ed.*, 2008, **47**, 452.